Chemical Physics 398 (2012) 154–159

Contents lists available at SciVerse ScienceDirect

Chemical Physics

journal homepage: www.elsevier.com/locate/chemphys

A set of cross sections and transport coefficients for electrons in HBr

O. Šašić [a,b,*], S. Dujko [a], T. Makabe [c], Z.Lj. Petrović [a]

[a] Institute of Physics, Belgrade, P.O. Box 68, 11080 Zemun, Belgrade, Serbia
[b] Faculty of Transport and Traffic Engineering, University of Belgrade, Vojvode Stepe 305, 11000 Belgrade, Serbia
[c] Department of Electronics and Electrical Engineering, Keio University, Hiyoshi 3-14-1, Yokohama, Japan

ARTICLE INFO

Article history:
Available online 26 August 2011

Keywords:
HBr
Swarms
Cross sections
Transport coefficients
Fluid models
Plasma etching

ABSTRACT

We have compiled a set of electron collision cross sections for HBr. It will be useful for a fluid modeling of HBr plasmas together with transport coefficients in both DC and RF, $\boldsymbol{E}$ and $\boldsymbol{E} \times \boldsymbol{B}$ fields. The calculation made use of a Monte Carlo technique. The transport coefficients are rather unstructured because the total cross section resembles that of a constant collisonal frequency model. Additional measurements of swarm parameters are required in order to obtain more acurate set of cross sections.

1. Introduction

Control of plasma chemistry and physical properties of ions reaching the surface as well as surface chemistry by radical species are critical to achieving appropriate functionality of plasma processing in the micro (nano) electronics industry [1,2]. In order to achieve proper adjustment of those properties, accurate and stable control of plasma reactors should be achieved. Contemporary plasma devices for nanoelectronic technologies are designed, modeled and understood and even operated by using equally complex plasma modeling codes. These plasma models [3–6] need to include atomic and molecular collision data base, electron ion and fast neutral transport data base, self consistent field calculation, general plasma physics stage, chemical kinetics of plasma, representation of boundaries between plasma and surfaces and also a section describing surface interactions and modifications. The surface set would have to involve modeling of the growth of structures, charging and also damage to the substrate and manufactured circuits. The foundation for the entire scheme is the set of cross sections and transport data.

Hydrogen bromide has been used in plasma processing of integrated circuits (ICs) for many different purposes [7–9] including: etching of poly Si [10–12], of III–V semiconductors [13], of high k gate dielectrics [14] and etching of low k oxides for interconnects [15].

HBr is used for plasma etching in various mixtures: combined with Ar [16], Br_2, F_2 [17], Cl_2 [10], with SF_6–O_2 [18,19], $SiCl_4$–SiF_4 [20], BCl_3, CH_4 [21], H_2, and even as a pure gas [13]. HBr was shown to possess all the required properties such as fast etching rate, selectivity and anisotropy except for side-wall passivation for etching applications [10,18,20,22–24]. Pushing into the realms of nanotechnologies control of etching induced surface roughness may prove to be critical [25,26].

In spite of the wide spread use and importance, to our knowledge, there have been no models of HBr-processes due to lack of basic electron collision and transport data. In some cases, when plasma models were developed, data for Cl_2 were used instead of HBr (with adjustment for the different mass ions) [27,28]. Thus it seemed to us that compiling a set of cross sections from the literature and adjusting them to form a complete (in terms of number, momentum and energy balances) set of data, together with the integrated transport data, would be a worthwhile endeavor. The data may prove to be useful for modeling plasmas involving HBr and reveal the basic characteristics of the transport coefficients. The present set of cross sections may encourage further experimental measurements needed to improve cross section and transport coefficient sets. Recent focus of the very few remaining swarm experiments has been towards gases used in applications [29] but one may need to develop a specialized apparatus for reactive gases in order to measure the data for gases like HBr. The calculations of the transport coefficients were made for DC electric fields and also for crossed $\boldsymbol{E}$ and $\boldsymbol{B}$, DC and RF fields. Preliminary reports of our work have been presented elsewhere [30,31].

2. The cross section data

Low energy elastic scattering by HBr molecules has not been the subject of many experiments, but there have been several theoretical studies [32–35]. The momentum transfer (and total elastic)

* Corresponding author at: Faculty of Transport and Traffic Engineering, University of Belgrade, Vojvode Stepe 305, 11000 Belgrade, Serbia. Tel.: +381 113091371.
E-mail addresses: o.sasic@sf.bg.ac.rs, vomsasic@open.telekom.rs (O. Šašić).

0301-0104/$ - see front matter © 2011 Elsevier B.V. All rights reserved.
doi:10.1016/j.chemphys.2011.08.019

cross sections in the energy range between 0.4 and 10 eV, that we have included in our set, were taken from Rescigno [36]. We extrapolated those results to high energies using Born's approximation (see Fig. 1). In order to provide the results for lower energies than 0.4 eV, we fitted the energy dependence of the cross sections for HCl to the HBr data.

In the region of low electron energies, the dominant features in the in elastic energy losses are vibrational excitation and dissociative attachment. Knowledge of these processes in the literature is much better than with those for other relevant cross section data [37–39]. We made use of the work of Horáček and coworkers [36]. These results are a combination of both theoretically and experimentally derived cross sections and the excellent agreement between them gives us confidence in both qualitative and quantitative features of the results.

As neither measurements nor calculations have been reported concerning the rotational excitation, we calculated the cross sections using the wellknown "Takayanagiformula" [40] which is applicable to molecules with large dipole moments. The results were normalized according to the populations of the corresponding states at the room temperature. Energy losses caused by these processes are very small but, as there are no other inelastic processes at such low energies (∼meV), it is important to include them in to the complete set of cross sections.

The effective total electronic excitation cross section rises rapidly from the threshold to a very broad peak around 30 eV, which is about eight times larger than the other peaks. We have adopted the results of calculations carried out by Rescigno [36] for dissociative excitation where all the states that correlate with the ground state atoms are included. Some necessary extrapolations towards higher energies were made using Born's approximation. Also the set was further enhanced with a fictitious or "effective total" excitation and ground state dissociation cross section adopted from a set of cross sections for HCl (Hayashi, personal communication, 1992). For ionization, we recommend the semi-empirical cross sections kindly calculated for us by the late Y.K. Kim (those results were later published [41]). The compiled set of cross sections is shown in Fig. 1.

The momentum transfer cross section is very large at low energies, which may be expected for a molecule with a significant dipole moment. The cross section decays with an energy dependence resembling that associated with a constant collision frequency. The Ramsauer–Townsend minimum in the elastic cross section occurs in the same energy region where vibrational excitation dominates. Additionally, there is a prominent threshold structure in the vibrational excitation cross section. The narrow threshold peak of the $v = 0 \rightarrow 1$ channel is of the order of 15×10^{-16} cm^2 and it is very close to the threshold peak for dissociative attachment, which is about three times smaller. It is greater by one or two orders of magnitude than those of typical gases used in plasma processing. The peaks of higher channels are much smaller and are also much wider.

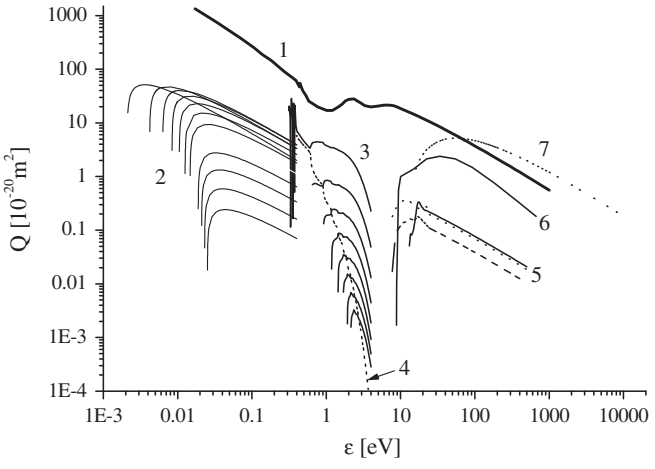

Fig. 1. Complete set of cross sections for HBr: 1, momentum transfer; 2, rotational excitation; 3, vibrational excitation; 4, dissociative attachment; 5, electronic excitation; 6, effective electronic excitation and dissociation; 7, ionization.

The proposed cross section set will be sufficient to calculate the transport coefficients. The present analysis shows a critical need for measurements of some transport coefficients, in particular ionization coefficients in order to obtain an improved set. Nevertheless, this set of cross sections should be quite reasonable for modeling of mixtures containing small amounts of HBr and good enough for plasma modeling in general.

3. Calculation technique

In this paper we use our Monte Carlo simulation code to calculate transport properties of electrons required as input in modeling of HBr plasma discharges. The code has been well tested and is described in great detail elsewhere [42–44]. Calculations are performed for constant and time varying electric fields and for crossed electric and magnetic fields having a 90° phase shift between the fields. The number of initial electrons in the simulations is set to 5×10^5 in order to provide good statistics for the output data and reasonable duration of our simulations. Our simulations usually lasted between 24 h and several days on the fastest personal computers. The initial electron velocity distribution function was Maxwellian with the mean starting energy of 1 eV but a sufficient number of collisions were allowed to achieve equilibrium between the energy input from the electric field and losses in collisions. The gas number density (N) in the simulations was 3.54×10^{22} m^{-3}, which corresponds to a pressure of 1 Torr (133.3 Pa) at a temperature of 273 K. Nevertheless, the results are of universal applicability as there are no non-hydrodynamic effects induced by the pressure dependent processes. In other words, the results presented in this study may be useful for all systems in equilibrium with the field until the density becomes sufficiently high (highly compressed gases and liquids) to introduce multiple simultaneous collisions [45]. After relaxation to the steady-state, the dynamic properties of an electron swarm are averaged over time and over all electrons in the simulation. As mean energies are predominantly in the region of a few eV, all electron scattering is assumed to be isotropic and, hence, the momentum transfer cross sections are used to represent the collisions. Under swarm conditions, the electron density is small enough that electron–electron interactions can be disregarded. The non-conservative nature of the ionization and attachment processes is carefully considered and, consequently, two sets of transport coefficients, the bulk and the flux, are derived. In the case of a DC electric field, in addition to the Monte Carlo calculations, transport coefficients are evaluated using the publicly available code ELENDIF [46] that solves the Boltzmann equation on the basis of two term approximation (TTA). In the case of HBr this approximation can be regarded as questionable due to the rapidly increasing cross sections for vibrational excitation in the same energy region where the cross section for momentum transfer in elastic collisions is a decreasing function of electron energy. Some of the results obtained using the TTA are compared with those obtained by the Monte Carlo simulation technique, primarily because of the simplicity of the technique and to illustrate once again the breakdown of the TTA for gases like HBr. In addition, the TTA is often used by the plasma modeling community and it is important to indicate the range of its applicability when calculation of drift and diffusion is of interest [47–49]. In this paper the TTA is used to obtain smooth curves in those E/N regions

where energy transfer in collisions is small and where the collisions have the effect of randomizing the direction of electron motion. This happens for very low E/N values where the accuracy of a Monte Carlo simulation is significantly reduced.

4. Results and discussion

4.1. Transport coefficients in DC electric fields

Fig. 2 shows the variation of the drift velocity with the reduced electric field (E/N), where 1 Td = 10^{-21} V m^2. We see that the drift velocity is a monotonically increasing function of E/N and negative differential conductivity (NDC) does not occur. NDC may have been expected due to sharp and rapidly decreasing cross sections for vibrational excitation that exceed the cross section for elastic scattering [50] and yet the almost constant collision frequency like energy dependence of the momentum transfer cross section leads to seemingly featureless profiles in the field dependence of the drift velocity. The explicit effects of non-conservative collisions can be clearly seen through a significant difference between the two sets (bulk and flux) of results. The bulk drift velocity is about 20% higher in the energy range where the ionization dominates the attachment processes. The ionization rate is an increasing function of electron energy, so electrons are predominantly created in regions of higher energies resulting in a forward shift of the center of mass position. Thus the bulk drift velocity increases with respect to the flux component. Conversely, in the range where the dissociative attachment is the most effective non-conservative process the bulk drift velocity is less than corresponding flux component. This follows from the energy dependence of the attachment rate coefficient. For electrons in HBr, and for E/N less than 70 Td, the attachment rate is proportional to the electron velocity. The more energetic electrons tend to be at the front of the swarm and are preferentially consumed. It follows that attachment will tend to move the center of mass of the swarm in the direction opposite to the drift. Thus the bulk drift speed decreases with respect to the flux component, as shown in Fig. 2.

When comparing results obtained in a MC simulation and those obtained by the TTA, we note a significant deviation between the two, particularly for lower E/N. For lower values of E/N, the large difference between MC and TTA results is not realistic and deserves more attention. We believe that this follows from the lack of sampling accuracy in simulating the rotational excitation and thermal effects in a MC simulation due to the excessive time consumption required for computation. The convergence of TTA and MC results around 70 Td indicates that there should be little difference between the two at lower E/N as confirmed by our calculations with identical cross section sets. In any case the difference between the TTA and MC results is never significant for drift velocities, but it is observable [47].

Fig. 3 displays the variation of the characteristic energy eD_T/μ with E/N. We observe that the inadequacies of the TTA are even more pronounced for eD_T/μ than for the drift velocity. This transport property clearly shows three regions that dominate the transport. The first initial slow rise for $E/N < 50$ Td follows from the significant energy losses due to vibrational excitation. Second, the rapid rise in eD_T/μ between 50 and 100 Td is a clear sign that the influence of the vibrational excitation is reduced. Finally, the following slow rise is a clear sign of the large energy loss as the inelastic channels including those for electronic excitation, dissociation and ionization become important. Perhaps the most striking property, however, is the behavior of the bulk and flux components. In contrast to the bulk and flux components of the drift velocity, we see that for lower E/N the bulk is greater than the flux component while for higher E/N the opposite is the case. The reason for this is that the flux component of the mobility decreases much faster with E/N in comparison with an increase in the bulk transverse diffusion coefficient with E/N. As a result of normalization, the flux values of eD_T/μ are greater than the corresponding bulk values when ionization is the most dominant non-conservative process and when the ionization collision frequency is a monotonically increasing function of electron energy.

The anisotropy of the diffusion is very weak, as shown in Fig. 4. For higher values of E/N the diffusion becomes isotropic. The degree of anisotropy has important implications for the anomalous behavior of the longitudinal diffusion coefficient in RF fields, as discussed in Section 4.3. The field dependence of diffusion coefficients for electrons in HBr is consistent with the theory of Parker and Lowke [51].

In Fig. 5 we show the ionization and attachment rates for electrons in HBr as functions of E/N. Typical operating conditions for most gaseous discharges and collisional plasmas are in the region where the energy losses caused by dissociative attachment are compensated by the production of free electrons by ionization. As can be seen from Fig. 5, the attachment and ionization rates intersect near 300 Td.

4.2. Transport coefficients in $\boldsymbol{E} \times \boldsymbol{B}$ DC fields

In this section we present the electron transport parameters in $\boldsymbol{E} \times \boldsymbol{B}$ DC fields. We consider the reduced electric field range: 50–2000 Td and the reduced magnetic field range: 100–3000 Hx

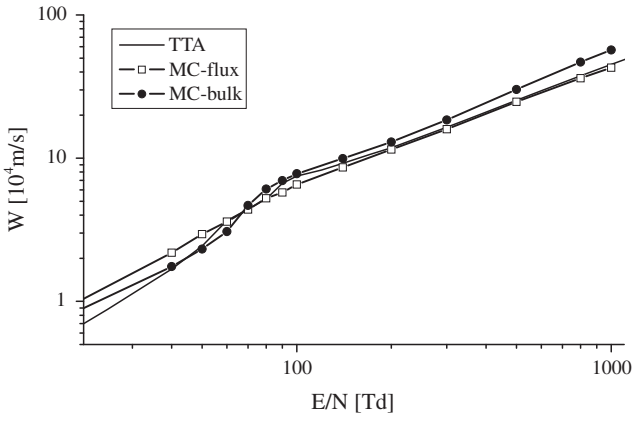

Fig. 2. Variation of the bulk and flux drift velocities with E/N for electrons in HBr. Results obtained from a MC simulation are compared with those obtained using the TTA for solving Boltzmann's equation.

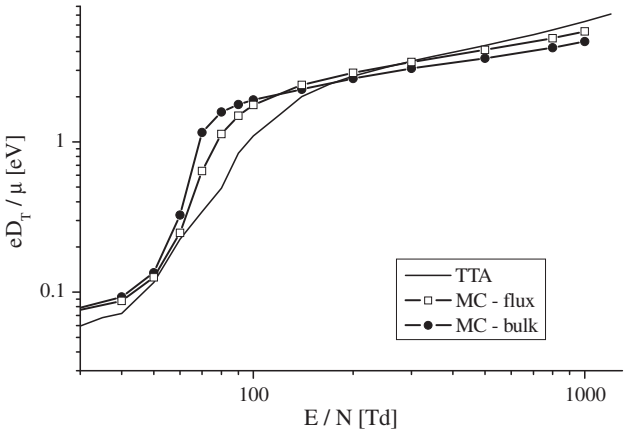

Fig. 3. Variations of the characteristic energy with E/N for electrons in HBr. Results obtained using a MC simulation are compared with those obtained from the TTA for solving Boltzmann's equation.

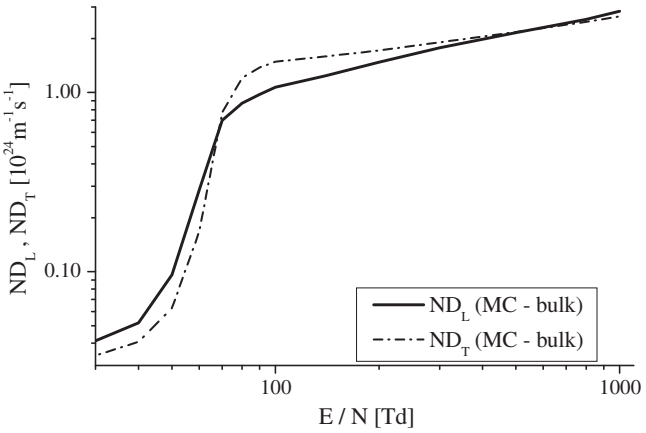

Fig. 4. Variation of the longitudinal and transverse diffusion coefficients for electrons in HBr.

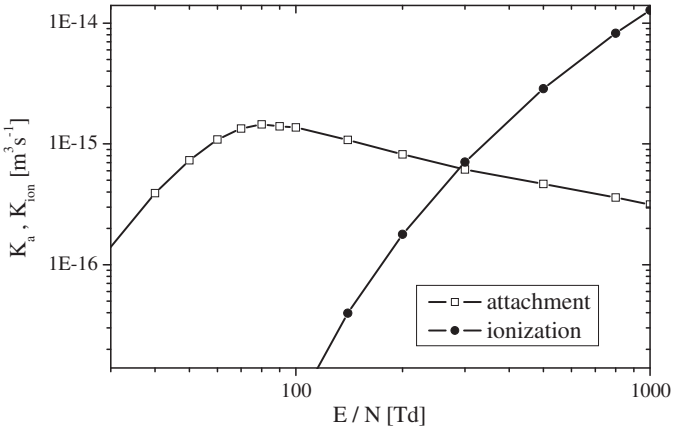

Fig. 5. Variation of the ionization and attachment rates with E/N for electrons in HBr.

(1 Hx = 10^{-27} T m^3). These conditions correspond to the collision dominated regime since the collision frequencies exceed the cyclotron frequencies in all cases because of the magnitude of the collision cross sections. The dependencies on E/N of the mean energy and drift velocity are similar to those obtained for the magnetic field free case except when the cyclotron frequency becomes comparable to the collision frequency. In general, the mean energy and drift velocity are decreasing functions of B/N. The profiles are shifted toward higher E/N, meaning a higher electric field is required to achieve the same mean energy and drift velocity. This follows from the well-known phenomenon of 'magnetic cooling' [52,53]. For E/N and B/N considered here, the profiles of the drift velocity are little affected by B/N and increase almost linearly (on a log–log scale) with E/N showing little sensitivity with respect to the energy dependence of the cross sections. The influence, however, of the magnetic field on the component of drift velocity in $\boldsymbol{E} \times \boldsymbol{B}$ direction is significant (see Fig. 6).

Diffusion coefficients show slightly higher sensitivity with respect to the energy dependence of cross sections. Namely, the E/N region where $ND_{\boldsymbol{E}\times\boldsymbol{B}}$ has a dramatic increment with E/N is the same region where the cross sections for vibrational excitation decrease and the cross section for momentum transfer in elastic collisions has a minimum (see Fig. 7). Beyond 200 Td the electronic excitation and ionization prevail and as they restrain diffusion so the coefficient rises only slowly. However, the fine structure of energy dependence of the cross sections is averaged out over the distribution function.

4.3. Transport coefficients in $E \times B$ RF fields

In this section we discuss the behavior of transport coefficients in $\boldsymbol{E} \times \boldsymbol{B}$ RF fields. The amplitudes of the applied electric fields are 100 and 500 Td. In order to study the effect of the amplitude of magnetic field, calculations were performed for the magnetic field free case and B/N of 100, 200, 500, 1000 and 2000 Hx while the frequency of the fields was fixed at 50 MHz. Furthermore, the temporal profiles of various transport parameters were investigated as a function of the field frequency (10, 50, 100, 500 and 1000 MHz) for the magnetic field free case and for a B/N of 1000 Hx. All relevant transport coefficients were calculated as well as the rate coefficients for all collision processes. In this paper we show only few of them but the rest will be available on-line [54].

In Figs. 8 and 9 we show the temporal variations of the longitudinal ($\boldsymbol{W}_{\boldsymbol{E}}$) and perpendicular ($\boldsymbol{W}_{\boldsymbol{E}\times\boldsymbol{B}}$) components of the drift velocity in crossed electric and magnetic fields for different amplitudes of the latter. As can be observed, the longitudinal component of drift velocity is little affected by the magnetic field, at least for amplitudes less than 500 Hx. The maximum values of $\boldsymbol{W}_{\boldsymbol{E}}$ do not depend on B/N as much as the positions of the peaks, which are centered for $B/N = 0$. There is also a phase delay in the $\boldsymbol{W}_{\boldsymbol{E}}$ curve relative to the electric field, which is more pronounced for larger magnetic fields. Furthermore, magnetic field affects the shape of the $\boldsymbol{W}_{\boldsymbol{E}}$ curve in such a way that, for the highest B/N, the shape is almost triangular.

The perpendicular ($\boldsymbol{W}_{\boldsymbol{E}\times\boldsymbol{B}}$) component of the drift velocity increases with B/N as does the asymmetry of the phase dependence (see Fig. 9). For the lowest B/N the positions of the peaks correspond to the peak of the $E(t)B(t)/E_0B_0$ function, but there is a clear change in the profiles for an increasing B/N. In addition, we see that the magnitudes of the peaks are not equal in the positive and negative directions, thus the mean value is not zero. This is a clear sign that magnetic field induces an effective force in the $\boldsymbol{E} \times \boldsymbol{B}$ direction producing a macroscopic drift in that direction while along the electric field direction the electrons simply oscillate around the initial positions [55].

In Fig. 10 we show the influence of field frequency on the drift velocity for the magnetic field free case. The modulation amplitude of the drift velocity decreases with the increment of the frequency, as expected, due to decrement of mean electron energy. The shapes of the drift velocity profiles are highly symmetric and sinusoidal with shifted phases for an increasing frequency. On the contrary, the behavior of the mean energy is much more dramatic with respect to frequency (not shown here). Namely, even for a slight increment of frequency, the mean energy significantly decreases and loses its modulation.

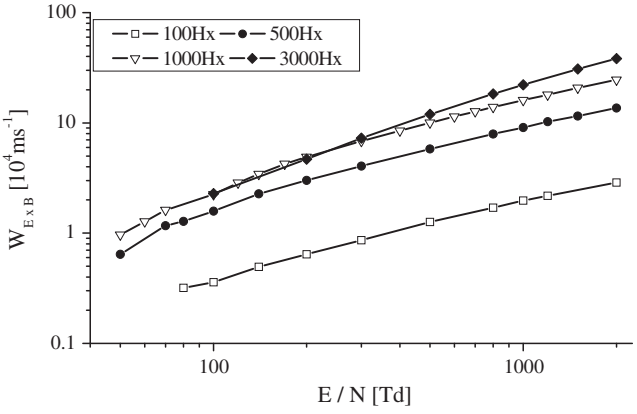

Fig. 6. Variation of the transverse component of the drift velocity with E/N and B/N for electrons in HBr in a crossed field configuration.

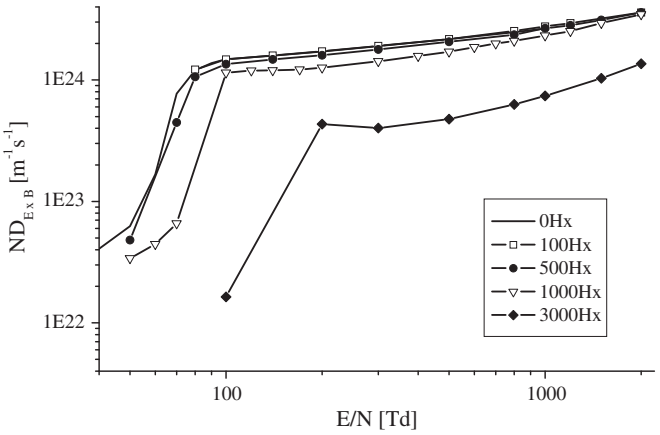

Fig. 7. Variation of the transverse diffusion coefficient along the $\boldsymbol{E} \times \boldsymbol{B}$ direction as a function of E/N and B/N for electrons in HBr.

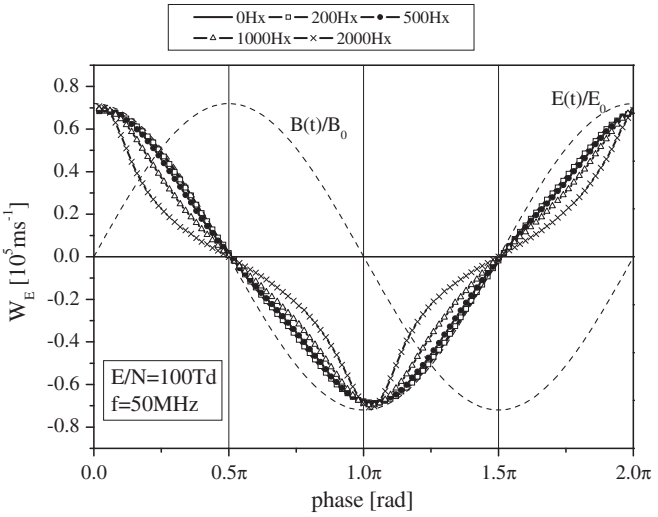

Fig. 8. Variation of the temporal profiles of the longitudinal drift velocity component with different amplitudes of magnetic field for electrons in HBr. The amplitude of the electric field is 100 Td and the frequency is 50 MHz.

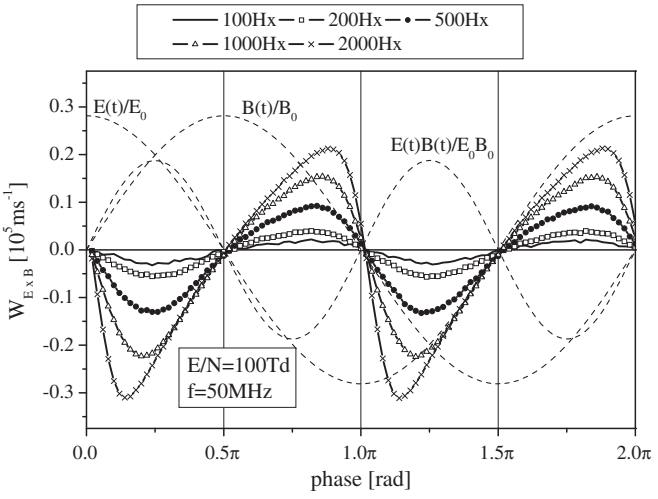

Fig. 9. Variation of the temporal profiles of the transverse drift velocity component with different amplitudes of magnetic field for electrons in HBr. The amplitude of the electric field is 100 Td and the frequency is 50 MHz.

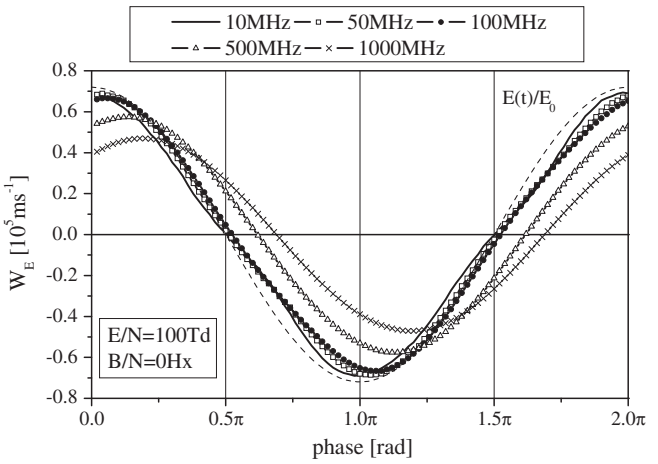

Fig. 10. Temporal profiles of the drift velocity for electrons in HBr in a time dependent electric field for various applied frequencies. The amplitude of the electric field is 100 Td.

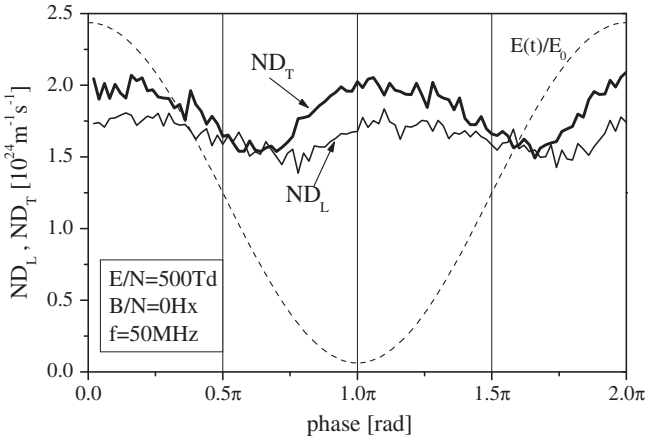

Fig. 11. Temporal profiles of the transverse (ND_T) and longitudinal (ND_L) components of the diffusion tensor for electrons in HBr in a time dependent electric field at 50 MHz. The amplitude of the electric field is 500 Td.

Calculated components of the diffusion tensor show only a slight anisotropy that changes with magnetic field and with frequency, as well. For low frequencies and no magnetic field, the cycle-averaged value of the transverse diffusion coefficient (ND_T) is somewhat higher than the longitudinal (ND_L), both coefficients are very modulated and nearly in phase with the field (see Fig. 11). ND_L increases with frequency, the modulation decreases, and, for the field frequency of 500 MHz, the diffusion is almost isotropic. At 1000 MHz ND_L becomes larger than ND_T when the electric field attains its peak value. When a magnetic field is applied, the diffusion coefficients decrease with an increment of magnetic field. Anomalous anisotropic behavior of the longitudinal diffusion coefficient [56,57] has not been observed.

5. Conclusion

We present a complete set of electron scattering cross sections in HBr that is compiled from the best available data in the literature. It is extended to a wider energy range and supplemented by an effective total excitation cross section. The main features are very large vibrational excitation and dissociative attachment cross sections and a Ramsauer–Townsend minimum in the elastic scattering cross section. If one wants to improve the set of cross sections, perhaps to the same degree of accuracy as is available

for other similar gases (e.g. HCl and Cl_2) further measurements of swarm parameters are needed, in particular ionization coefficients, characteristic energies and drift velocities. In addition, more studies of electronic excitation and dissociation are needed in order to normalize this cross section set and integrate processes that have not been treated herein. However, this set of cross sections should work well for modeling collisional plasmas in gas mixtures containing smaller amounts of HBr.

In addition to cross sections, we have calculated a set of transport coefficients and collisional rates using Monte Carlo simulations of electron transport under conditions of constant and time varying electric and crossed electric and magnetic fields. Our results suggest that a magnetic field strongly affects the electron transport producing complex behavior, which consequently means that standard approximations such as the effective field approximation and instantaneous field approximation are dubious in plasma models [1,43].

Our calculations show that the diffusion of electrons is only slightly anisotropic. The absence of interesting kinetic phenomena, such as negative differential conductivity or anomalous anisotropic behavior of the longitudinal diffusion coefficient in time-dependent fields, is due to a very weak energy dependence of the total collision frequency.

Assuming that the measured and calculated cross sections are as presented, the following holds for the present set:

- at lower energies (below 4 eV) both momentum and energy balances are well represented by accurate cross sections and the bulk of electrons in typical plasmas would be modeled very well;
- at higher energies the most serious problem is the lack of information needed to determine overall energy losses, which have been compensated by an effective dissociation cross section based on the data available for HCl.

This means that in mixtures, even with rare gases, the momentum and energy balance will be well established. At higher energies, however, the inaccuracy of the dissociation cross section is in competition with the energy loss processes in the more abundant buffer gas and does not pose a problem. The only situation where the set would appear inadequate is for pure HBr at higher energies [47,48].

Measurement of the ionization rate for HBr or its mixtures would help to normalize the cross sections having thresholds close but below the threshold for ionization. These processes, including electronic excitation and dissociation, determine the electron energy distribution function in the region of overlap with the ionization cross section and thus the rate for ionization is much more sensitive to those processes than to ionization cross section itself [47,48]. Measurements of rates for all other inelastic processes would help resolve details of the energy and momentum balances, but the critical set of data that we need at present is the ionization rate. The accuracy required for plasma modeling [1] is such that the present compilation of cross sections and transport coefficients provides sufficient accuracy for this very important gas.

Acknowledgements

This work was funded by the MES ON171037 and II41011projects. Authors are grateful to J. Horáček, M. Allan and the late Yong-Ki Kim for sending us their data some prior to publication and to the two referees for helping us improve the presentation of the paper.

References

[1] T. Makabe, Z.Lj. Petrović, Plasma Electronics: Applications in Microelectronic Device Fabrication, Taylor and Francis, New York, 2006.
[2] M.A. Lieberman, A.J. Lichtenberg, Principles of Plasma Discharges and Materials Processing, second ed., Wiley, Wiley Interscience, Hoboken, NJ, 2005.
[3] T. Makabe, K. Maeshige, Appl. Surf. Sci. 192 (2002) 176.
[4] F. Hamaoka, T. Yagisawa, T. Makabe, J. Phys.: Conf. Ser. 86 (2007) 012018.
[5] M.J. Kushner, J. Phys. D 42 (2009) 194013.
[6] T. Makabe, T. Tatsumi, Plasma Sources Sci. Technol. 20 (2011) 024014.
[7] T.D. Bestwick, G.S. Oehrlein, Y. Zhang, G.M.W. Kroesen, E. de Fresart, Appl. Phys. Lett. 59 (1991) 336.
[8] S. Xu, T. Sun, D. Podlesnik, J. Vac. Sci. Technol. A 19 (2001) 2893.
[9] L. Desvoivres, L. Vallier, O. Joubert, J. Vac. Sci. Technol. B 19 (2001) 420.
[10] K.M. Chang, T.H. Yeh, I.C. Deng, H.C. Lin, J. Appl. Phys. 80 (1996) 3048.
[11] S.A. Vitale, H. Chae, H.H. Sawin, J. Vac. Sci. Technol. A 19 (2001) 2197.
[12] S. Bouchoule, G. Patriarche, S. Guilet, L. Gatilova, L. Largeau, P. Chabert, J. Vac. Sci. Technol. B 26 (2008) 666.
[13] S. Vicknesh, A. Ramam, J. Electrochem. Soc. 151 (2004) C772.
[14] S. Agarwala, I. Adesida, C. Caneau, R. Bhat, Appl. Phys. Lett. 62 (1993) 2830.
[15] S.A. Vitale, H.H. Sawin, J. Vac. Sci. Technol. A 20 (2002) 651.
[16] S.J. Pearton, U.K. Chakrabarti, E. Lane, A.P. Perley, C.R. Abernathy, W.S. Hobson, J. Electrochem. Soc. 139 (1992) 856.
[17] H. Takazava, H. Takatani, S. Yamamoto, Jpn. J. Appl. Phys. 35 (1996) L754.
[18] S. Gomez, R. Jun Belen, M. Kiehlbauch, E.S. Aydila, J. Vac. Sci. Technol. A 23 (2005) 1592.
[19] E. Pargon, O. Joubert, T. Chevolleau, G. Cunge, Songlin Xu, T. Lill, J. Vac. Sci. Technol. B 23 (2005) 103.
[20] S.K. Murad, S.P. Beaumont, C.D.W. Wilkinson, Appl. Phys. Lett. 67 (1995) 2660.
[21] Y. Kuo, T.L. Tai, J. Electrochem. Soc. 145 (1998) 4313.
[22] C.C. Cheng, K.V. Guinn, V.M. Donnelly, J. Vac. Sci. Technol. B 14 (1996) 85.
[23] I. Tepermeister, N. Blayo, F.P. Klemens, D.E. Ibbotson, R.A. Gottscho, J.T.C. Lee, H.H. Sawin, J. Vac. Sci. Technol. B 12 (1994) 2310.
[24] H. Ohtake, K. Noguchi, S. Samukawa, H. Iida, A. Sato, X.Y. Qian, J. Vac. Sci. Technol. B 18 (2000) 2495.
[25] M. Martin, G. Cunge, J. Vac. Sci. Technol. B 26 (2008) 1281L.
[26] L. Vallier, J. Foucher, X. Detter, E. Pargon, O. Joubert, G. Cunge, T. Lill, J. Vac. Sci. Technol. B 21 (2003) 904.
[27] H.H. Hwang, M. Meyyappan, G.S. Mathad, R. Ranade, J. Vac. Sci. Technol. B 20 (2002) 2199.
[28] M.A. Vyvoda, M. Li, D.B. Graves, H. Lee, M.V. Malyshev, F.P. Klemens, J.T.C. Lee, V.M. Donnelly, J. Vac. Sci. Technol. B 18 (2000) 820.
[29] O. Šašić, J. de Urquijo, A.M. Juarez, S. Dupljanin, J. Jovanović, J.L. Hernandez-Avila, E. Basurto, Z.Lj. Petrović, Plasma Sources Sci. Technol. 19 (2010) 034003.
[30] O. Šašić, Z.Lj. Petrović, Rad. Phys. Chem. 76 (3) (2007) 573.
[31] O. Šašić, S. Dujko, Z.Lj. Petrović, T. Makabe, Jpn. J. Appl. Phys. 46 (6A) (2007) 3560.
[32] Y. Itikawa, Phys. Rep. 46 (1978) 117.
[33] H. Estrada, W. Domcke, J. Phys. B 17 (1984) 279.
[34] L. Malegat, M. Le Dourneuf, J. Phys. B: At. Mol. Opt. Phys. 23 (1990) 527.
[35] R. Fandreyer, P.G. Burke, L.A. Morgan, C.J. Gillan, J. Phys. B 26 (1993) 3625.
[36] T.N. Rescigno, J. Chem. Phys. 104 (1996) 125.
[37] K. Rohr, J. Phys. B 11 (1978) 1849.
[38] J. Horáček, W. Domcke, Phys. Rev. A 53 (1996) 2262.
[39] M. Čižek, J. Horáček, A. Sergenton, D. Popović, M. Allan, W. Domcke, T. Leininger, F. Gadea, Phys. Rev. A 63 (2001) 062710.
[40] K. Takayanagi, Phys. Soc. Jpn. 21 (1966) 507.
[41] M.A. Ali, Y.K. Kim, J. Phys. B, At. Mol. Opt. Phys. 41 (2008) 145202.
[42] S. Bzenić, Z.M. Raspopović, S. Sakadžić, Z.Lj. Petrović, IEEE Trans. Plasma Sci. 27 (1999) 78.
[43] Z.Lj. Petrović, Z.M. Raspopović, S. Dujko, T. Makabe, Appl. Surf. Sci. 192 (2002) 1.
[44] S. Dujko, Z.M. Raspopović, Z.Lj. Petrović, J. Phys. D: Appl. Phys. 38 (2005) 2952.
[45] R.D. White, R.E. Robson, Phys. Rev. Lett. 102 (2009) 230602.
[46] W.L. Morgan, B.M. Penetrante, Comp. Phys. Commun. 58 (1990) 127.
[47] Z.Lj. Petrović, S. Dujko, D. Marić, G. Malović, Ž. Nikitović, O. Šašić, J. Jovanović, V. Stojanović, M. Radmilović-Rađenović, J. Phys. D: Appl. Phys. 42 (19) (2009) 194002.
[48] Z.Lj. Petrović, M. Šuvakov, Ž. Nikitović, S. Dujko, O. Šašić, J. Jovanović, G. Malović, V. Stojanović, Plasma Sources Sci. Technol. 16 (2007) S1.
[49] R.D. White, R.E. Robson, B. Schmidt, M.A. Morrison, J. Phys. D: Appl. Phys. 36 (2003) 3125.
[50] Z.Lj. Petrović, R.W. Crompton, G.N. Haddad, Aust. J. Phys. 37 (1984) 23.
[51] J.H. Parker, J.J. Lowke, Phys. Rev. 181 (1969) 290.
[52] K.F. Ness, J. Phys. D: Appl. Phys. 27 (1994) 1848.
[53] S. Dujko, R.D. White, K.F. Ness, Z.Lj. Petrovic, R.E. Robson, J. Phys. D: Appl. Phys. 39 (2006) 4788.
[54] http://mail.ipb.ac.rs/~cep/ipb-cnp/ionsweb/database.htm.
[55] Z.M. Raspopović, S. Dujko, T. Makabe, Z.Lj. Petrović, Plasma Sources Sci. Technol. 14 (2005) 293.
[56] K. Maeda, T. Makabe, N. Nakano, S. Bzenić, Z.Lj. Petrović, Phys. Rev. E 55 (1997) 5901.
[57] R.D. White, R.E. Robson, K.F. Ness, Aust. J. Phys. 48 (1995) 925.